



# Complementary analyses of a tricalcium silicate sample hydrated at high pressure and temperature

Fabienne Méducin<sup>a,\*</sup>, Christine Noïk<sup>b</sup>, Alain Rivereau<sup>b</sup>, Hélène Zanni<sup>a</sup>

<sup>a</sup>Laboratoire de Physique et Mécanique des Milieux Hétérogènes, UMR CNRS 7636, Ecole Supérieure de Physique et Chimie Industrielles, 10 rue Vauquelin, 75231 Paris Cedex 05, France

<sup>b</sup>Institut Français du Pétrole, BP 311, 1 et 4 avenue de Bois Préau, 92506 Rueil-Malmaison Cedex, France

Received 27 October 2000; accepted 24 July 2001

## Abstract

A cement slurry is universally used to support the casing of oilwells. Cementing operations consist in placing an appropriate cement slurry in the annulus between the walls of the hole and the casing that has been run in. This slurry is pumped down the steel casing of the well and then placed in the annular space between the casing and the surrounding rock. Nowadays, wells become deeper and deeper—at least 6 km length—so the setting conditions of the cement paste are drastic. Pressure and temperature may reach 1000 bars and 350 °C at the bottom of the well. Hydration of synthetic tricalcium silicate—main component of oilwell cements—was performed at high temperature under a high pressure to simulate the oilwell conditions. In these unusual setting conditions, a mixture of different silicate hydrates was synthesized and was rather difficult to analyse and quantify. So, DTA, TG, NMR, XRD and SEM techniques were used to study the cement hydration process. The complementarity of all these techniques was pointed out for the investigations on cementitious materials, more specially, on a sample hydrated at 200 °C under a pressure of 450 bars during 2 months. © 2002 Elsevier Science Ltd. All rights reserved.

**Keywords:** Hydration; Scanning electron microscopy; X-rays diffraction; Spectroscopy;  $\text{Ca}_3\text{SiO}_5$

## 1. Introduction

The general objective of this study is to understand  $\text{Ca}_3\text{SiO}_5$  hydration in order to establish an updated phase diagram of  $\text{Ca}_3\text{SiO}_5/\text{H}_2\text{O}$ . Correlation between the structure, the morphology and the mechanical properties of the hydrated phases is considered. The results concerning one sample hydrated at 200 °C under 450 bars during 2 months are discussed in this paper.

In the cement chemistry notation system generally used by the cement and concrete industry, C stands for CaO, S for  $\text{SiO}_2$  and H for  $\text{H}_2\text{O}$  [1]. So tricalcium silicate  $\text{Ca}_3\text{SiO}_5$  is also called  $\text{C}_3\text{S}$ . Oilwell cements are Portland cements often of Class G, defined on the American Petroleum Institute standard, API specification 10 [2], standard similar to the ISO 10426-1 and similar to the ASTM II type. This class G for the high sulphate resistant type is mainly composed of silicate phases with a maximum of 65%  $\text{C}_3\text{S}$  and of 20%

$\text{C}_2\text{S}$  and of aluminates phases ( $\text{C}_4\text{AF}$ ,  $\text{C}_3\text{A}$ ) at a maximum of 25%. During cementing operation in oilwell, the cement slurry is pumped down the steel casing of the well and then placed in the annular space between the casing and the surrounding rock to support the casing.

Masse and Bresson [3,4] have already determined the structure evolution of calcium silicate hydrates formed up to 160 °C and the effect of pressures up to 1000 bars in certain cases. The present study has focused on the hydrated system ( $\text{C}_3\text{S}/\text{H}$ ) at higher temperature and pressure in order to simulate setting conditions in deeper oilwells. Synthetic Tricalcium silicate  $\text{C}_3\text{S}$  has been used. Previous studies [2,5] have shown that nuclear magnetic resonance spectroscopy (NMR), in association with X-ray diffraction analysis (XRD) and scanning electron microscopy (SEM), are useful techniques for the detection of the constituent phases of a silicate matrix. The detection of calcium silicate hydrates could be performed through XRD and thermal analysis for all the crystalline phases. NMR permits both the confirmation of the presence of highly structured phases and the detection of poorly crystallized phases. Then, the morphology of each phase is determined with SEM through local

\* Corresponding author. Tel.: +33-1-40-79-45-56; fax: +33-1-40-79-47-95.

E-mail address: fmeducin@pmmh.espci.fr (F. Méducin).

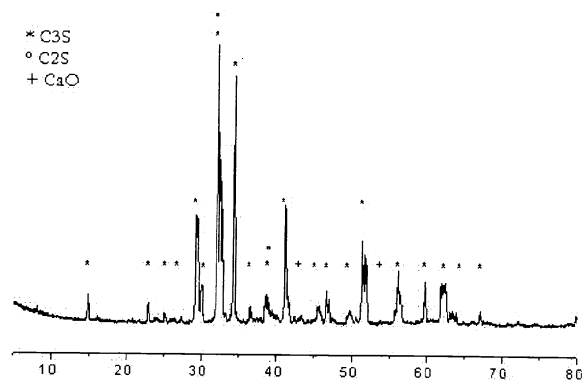


Fig. 1. Diffraction pattern of synthetic  $C_3S$  (triclinic structure).

observations coupled with electron dispersive X-ray analysis. The main problem of quantification can be solved through thermal analysis and particularly through  $^1H$ - and  $^{29}Si$ -NMR investigations.

## 2. Experimental

### 2.1. Sample preparation

The quality of synthetic  $C_3S$  (triclinic T1 structure) have been verified by various methods. Among them, XRD (Fig. 1) allowed us to evidence a little amount of  $CaO$  (1.1% determined by chemical way too) and  $C_2S$  (<1%, revealed by NMR technique too). In order to reproduce the conditions of a deep oilwell, synthetic  $C_3S$  has been prepared at room temperature with a water/cement (W/C) ratio of 0.44, the standard consistency requirement of class G cement. Distilled water was used here. Then, a Teflon pot filled up with this cement paste was placed in distilled water in a high temperature and pressure cell. Oil was the pressure transmitting fluid. The pressure was regulated first, then the external heating began once the pressure was effective. The pressure and temperature stable conditions were reached after three hours. And the silicate sample was left in the cell in order to cure during 2 months at 200 °C under 450 bars.

### 2.2. Analyses

The considered sample of hydrated tricalcium silicate has been studied by a set of methods. First, the crystalline phases have been detected by XRD on a Philips PW 1820 device equipment. XRD experiment was performed with powdered sample. The diffraction pattern was performed from  $2\theta = 10^\circ$  to  $80^\circ$  with a step of  $0.03^\circ$  and 4 s per step.

Then, thermal analysis was performed, with a thermobalance TAG24 SETARAM, in order to confirm the XRD results and quantify the different phases. After being weighed (exactly 42.74 mg), the powdered sample was submitted to a raise in temperature ranging from 20 °C up

to 1050 °C with a 10 °C/min rate. Meanwhile, the weight loss was recorded.

In addition, SEM and energy dispersive X-ray spectrometer (SEM-EDX), were used to observe the morphology of the hydrated tricalcium silicate. Secondary electron images of fractures and qualitative X-rays analyses were performed on a JEOL 6300F field emission electron microscope fitted with a IMIX PGT EDS spectrometer. The sample is first covered by a thin metallic layer of platinum to increase the poor conductivity of the observed fracture. The observation takes place in a  $4 \times 10^{-6}$  Torr vacuum and a high acceleration tension (15 kV).

At last,  $^{29}Si$ - then  $^1H$ -NMR were used to determine the validity of the first results and to probe amorphous or poorly crystallized phases possibly present. The sample with  $^{29}Si$  isotopic natural abundance (4.7%) was investigated through an ASX 300 Bruker spectrometer at a resonance frequency of 59.6 MHz. The pulse sequences used—MAS Single Pulse and  $^1H$ - $^{29}Si$  CPMAS (cross-polarization at magic angle spinning)—are well known for solid-state NMR studies [6,7]. The resolution is optimized with the signal of  $Q_8M_8$   $[Si(CH_3)_3]_8Si_8O_{20}$ , which was used as reference for the chemical shift measurement too. The calibration gives the biggest peak at 11.6 ppm. MAS Single Pulse and CPMAS experiments were performed with the following parameters: a  $\pi/2$  pulse length of 3.3  $\mu s$ , a spinning frequency of 5 kHz. A Single Pulse experiment was achieved with a recycle delay of 150 s and 470 scans of accumulation. The C-S-H relaxation— $T_1 = 30$  s—was respected, provided C-S-H [1] was present in this hydrated sample. A number of scans equal to 10000, a recycle delay of 5 s and a contact time ranging from 1 to 10 ms were used in the CPMAS experiments. With these CPMAS experiments the dynamics of polarization of each phase are clearly evidenced in agreement with previous work [4]. Moreover, NMR experiments permit us to validate the first attempt of quantification performed with thermal analysis.  $^1H$ -NMR Experiments were performed on an ASX 300 Bruker

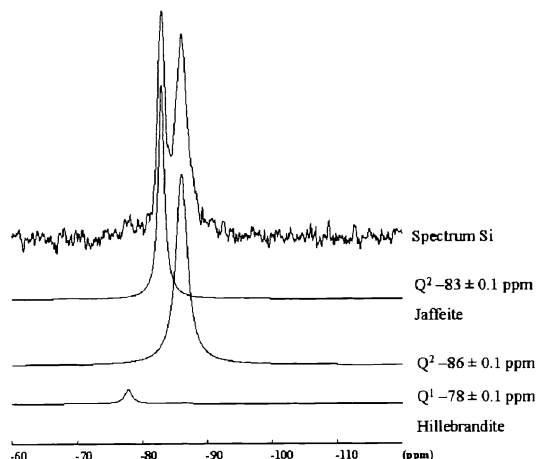


Fig. 2. Single pulse experiment spectrum ( $^{29}Si$ ) of the  $C_3S$  hydrated sample (W/C=0.44) at 200 °C under 450 bars during 2 months.

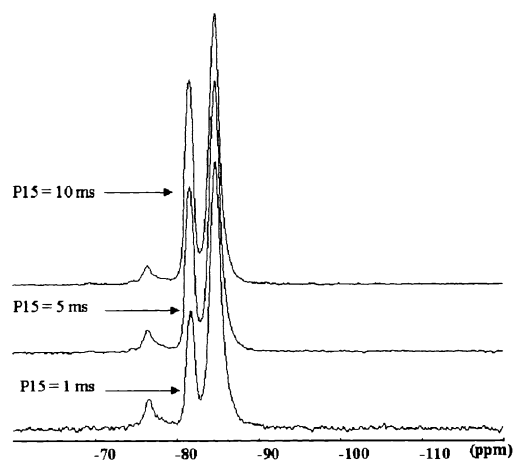


Fig. 3.  $^1\text{H}$ – $^{29}\text{Si}$  CP experiments spectra (contact time P15 values: 1–10 ms) of the  $\text{C}_3\text{S}$  hydrated sample ( $\text{W/C}=0.44$ ) at  $200^\circ\text{C}$  under 450 bars during 2 months.

spectrometer at a resonance frequency of 300 MHz on a sample with  $^1\text{H}$  isotopic natural abundance ( $\sim 100\%$ ). The pulse sequence used—CRAMPS (combined rotation and multipulse spectroscopy) [8]—is well known for solid-state  $^1\text{H}$ -NMR studies [9,10]. It permits removal of the homonuclear proton–proton dipolar interaction, which broadens the peaks in MAS  $^1\text{H}$ -NMR experiments. Resolution and calibration are adjusted with the signal of adamantane  $\text{C}_{10}\text{H}_{16}$ , with a peak at 1.7 ppm.

### 3. Results

#### 3.1. Phases detection

X-rays powder diffraction allows us to find three main phases in agreement with the technical literature (JCPDS data 44–1481, 29–375 and 42–538 pattern): portlandite CH, jaffeite  $\text{Ca}_6(\text{Si}_2\text{O}_7)(\text{OH})_6$  also called tricalcium silicate hydrate TCSH, with the chemistry oxides notation, and hillebrandite  $\text{Ca}_2(\text{SiO}_3)(\text{OH})_2$  also called  $\text{C}_2\text{SH}$ . But hillebrandite is not the  $\alpha$ -polymorph well known for its very low mechanical resistance due to a layered structure [11,12]. We can also observe some calcite  $\text{CaCO}_3$  formed when

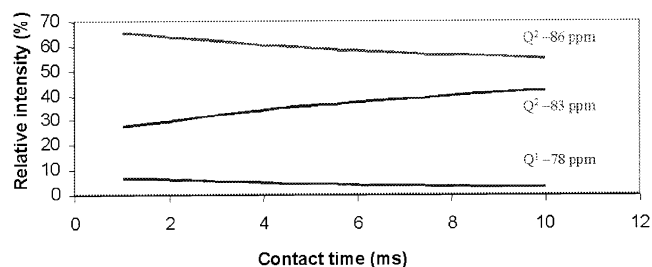


Fig. 4. Relative intensity of CP-peaks (%) as a function of contact time value between  $^1\text{H}$  and  $^{29}\text{Si}$  (1–10 ms) of the  $\text{C}_3\text{S}$  hydrated sample ( $\text{W/C}=0.44$ ) at  $200^\circ\text{C}$  under 450 bars during 2 months.

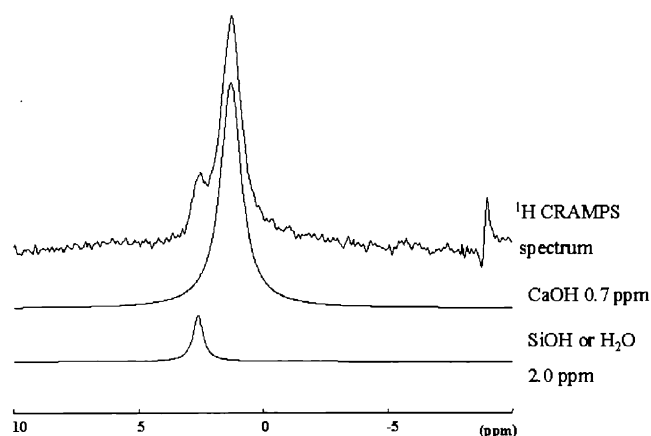


Fig. 5. Pure synthetic hillebrandite CRAMPS spectrum ( $^1\text{H}$ ).

contact with air during the sample conditioning required for the analysis.

However, XRD is unable to investigate amorphous or poorly crystallized phases. In particular, nonstoichiometric phases like C–S–H [1,13] are potentially present but cannot be clearly detected by this method.

Thermal analysis confirms the trends observed by X-ray diffraction studies. Three endothermic peaks could be identified: one at  $65^\circ\text{C}$  corresponding to the loss of physically adsorbed water, the second one at  $448^\circ\text{C}$  characteristic of constituent water of portlandite (CH) and the last one at  $531^\circ\text{C}$  representing the loss of constituent water of jaffeite ( $\text{C}_6\text{S}_2\text{H}_3$ ).

Then  $^{29}\text{Si}$ -NMR experiments were performed to detect whether some amorphous or poorly crystallized phases have been formed during hydration. The spectra are shown in Figs. 2 and 3. In Fig. 2, the Single Pulse experiment spectrum, two main peaks are observed at around  $-83.0 \pm 0.1$  ppm (corresponding to  $\text{Q}^2$  entities, i.e.,  $\text{SiO}_4$  tetrahedra in the middle of silicate chains) and  $-86.0 \pm 0.1$  ppm (corresponding to  $\text{Q}^2$  entities), according to Michel and Engelhardt's chemical shift table [14]. A third little peak at about  $-78.0 \pm 0.1$  ppm corresponds to  $\text{Q}^1$  entities, tetrahedra at the end of silicate chains. These

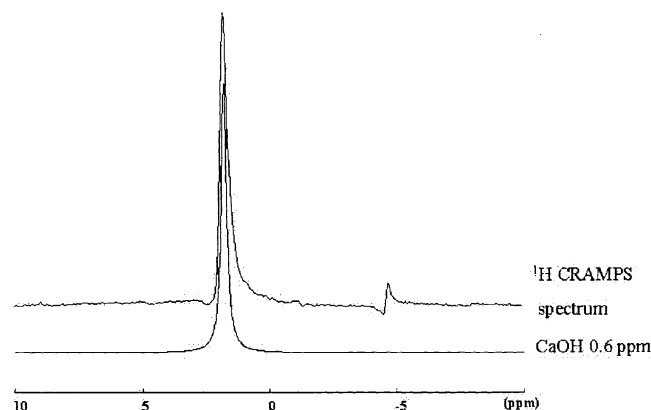


Fig. 6. Pure synthetic portlandite CRAMPS spectrum ( $^1\text{H}$ ).

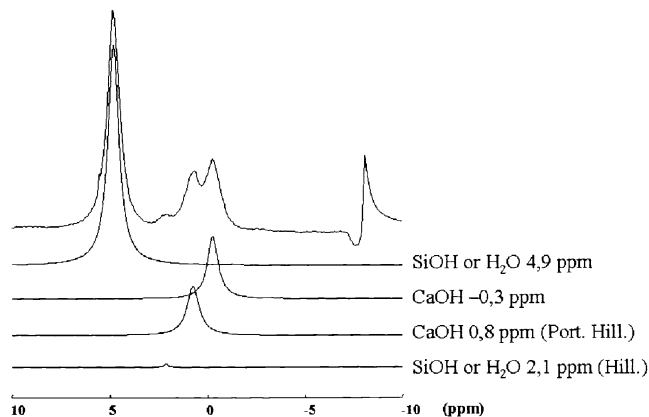


Fig. 7. CRAMPS spectrum ( $^1\text{H}$ ) of the  $\text{C}_3\text{S}$  hydrated sample ( $\text{W/C}=0.44$ ) at  $200^\circ\text{C}$  under 450 bars during 2 months.

peaks are not very broad showing that the phases observed are quite well crystallized. The half-height width is only 1 or 2 ppm here. In the case of the amorphous phases, this half-height width can reach 3 or 4 ppm. The XRD results have shown that four crystalline phases can be found, two of them containing silicon: jaffeite and hillebrandite.

CPMAS experiments at different contact times (1, 5 and 10 ms) were meant to highlight the presence of these two phases, as was done by B. Bresson, with many more contact times [4]. In Fig. 3, we can observe the CPMAS spectra with three peaks at around  $-78.0 \pm 0.1$  ppm ( $\text{Q}^1$  entities),  $-83.0 \pm 0.1$  ppm ( $\text{Q}^2$  entities) and  $-86.0 \pm 0.1$  ppm ( $\text{Q}^2$  entities). When the relative intensity is given as a function of the contact time between  $^1\text{H}$  and  $^{29}\text{Si}$ , it was observed firstly that the same trend of relaxation dynamic for the peaks at  $-78.0 \pm 0.1$  and  $-86.0 \pm 0.1$  ppm arose, showing that these  $\text{Q}^1$  and  $\text{Q}^2$  entities belong to the same phase (Fig. 4). The  $\text{Q}^2$  entities at  $-83.0 \pm 0.1$  ppm come from another phase with different relaxation dynamic. These CPMAS experiments were performed with only three contact times in order to observe only the trend of the relax-

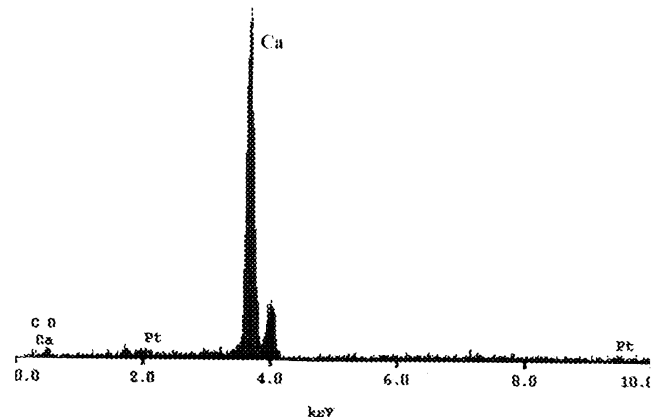


Fig. 9. Electron dispersive X-ray analysis of the blocs (portlandite:  $\text{Ca}(\text{OH})_2$ ) of the  $\text{C}_3\text{S}$  hydrated sample ( $\text{W/C}=0.44$ ) at  $200^\circ\text{C}$  under 450 bars during 2 months.

ation dynamic. Previous investigations have proved that this second phase is jaffeite [4]. Thus, the other phase determined is hillebrandite (peaks at  $-78.0 \pm 0.1$  and  $-86.0 \pm 0.1$  ppm). Chemical shifts for the two phases are in agreement with the literature: Bell et al. [15] found a main peak for hillebrandite at  $-86.0$  ppm and Bresson has found a peak at  $-82.7$  ppm for the jaffeite.

At least,  $^1\text{H}$ -NMR experiments were performed to confirm the presence of all the observed phases, as did  $^{29}\text{Si}$ -NMR experiments. First,  $^1\text{H}$  CRAMPS spectra of pure hillebrandite and pure portlandite (synthetic phases) are given in Figs. 5 and 6, with the corresponding simulated lines. Two peaks are to be found (Fig. 5) for hillebrandite at  $0.7 \pm 0.1$  (relative to  $\text{CaO-H}$  groups) and  $2.0 \pm 0.1$  ppm (relative to  $\text{H-OH}$  or  $\text{SiO-H}$  groups) according to Heide-mann's chemical shift table [16]. One peak, relative to  $\text{CaO-H}$  groups, appears for portlandite at  $0.6 \pm 0.1$  ppm as shown on Fig. 6. The artifact at around  $-5$  or  $-10$  ppm is due to the irradiation frequency.



Fig. 8. SEM image of secondary electrons of the  $\text{C}_3\text{S}$  hydrated sample ( $\text{W/C}=0.44$ ) at  $200^\circ\text{C}$  under 450 bars during 2 months ( $\times 350$ ).

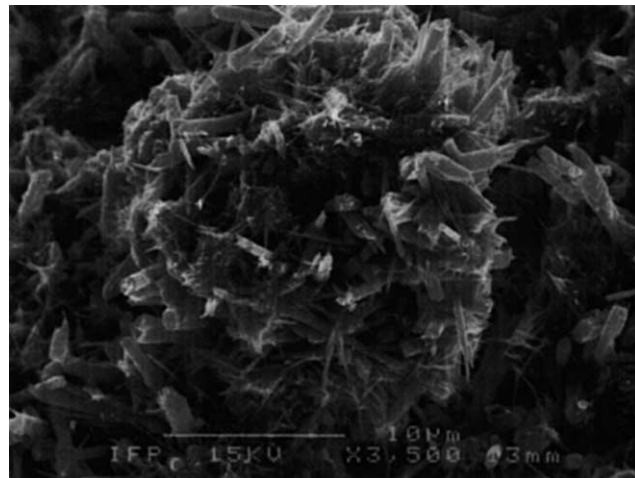


Fig. 10. SEM image of secondary electrons ( $\times 3500$ ) of the  $\text{C}_3\text{S}$  hydrated sample ( $\text{W/C}=0.44$ ) at  $200^\circ\text{C}$  under 450 bars during 2 months.

With those references, the CRAMPS spectrum of the sample (Fig. 7) can clearly be analyzed. The latter peaks correspond to proton groups in hillebrandite ( $0.8 \pm 0.1$  and  $2.1 \pm 0.1$  ppm) and portlandite ( $0.8 \pm 0.1$  ppm). The other peaks thus come from jaffeite ( $-0.3 \pm 0.1$  and  $4.9 \pm 0.1$  ppm), which is the only other hydrogenated phase present.

### 3.2. Phases morphology

The morphology of the hydrated tricalcium silicate was studied by SEM using secondary electrons. In Fig. 8, a fibrillary phase can be highlight, which can only be jaffeite. Blocks of portlandite, the composition of which was determined by dispersive X-ray analysis (Fig. 9), are also to be found here. This analysis is only qualitative but clearly shows that there is no silicon in these blocks, only Ca and O (H is not detected). A continuous phase (Fig. 10) with a woolly aspect is observed, which is most likely to be hillebrandite, in agreement with the electron dispersive X-ray analysis. This morphology is close to the C–S–H morphology, a sea urchin with numerous disordered needles. Moreover, the peaks position of  $^{29}\text{Si}$ -NMR for these two phases are close, about  $-79.3 \pm 0.1$  and  $-85.6 \pm 0.1$  ppm for C–S–H and  $-78.0 \pm 0.1$  and  $-86.0 \pm 0.1$  ppm for hillebrandite.

### 3.3. Phases quantification

The weight of each phase can be deduced from the corresponding weight loss of water, reported to the molecular weight of the considered phase. The most reliable result is obtained for portlandite:  $\sim 13 \pm 1\%$  of portlandite was obtained for our sample by thermal analysis. A Single Pulse Experiment (with respect of the longer relaxation time) enables the quantification of the relative amounts of the two silicon containing phases (jaffeite and hillebrandite). The surface area under each peak is proportional to the amount of silicon contained in each phase. The molecular weight of each considered phase taken into account leads to a weight ratio jaffeite/hillebrandite  $\sim 0.8$ . Moreover, the  $^1\text{H}$ -NMR CRAMPS technique provides quantitative results. The computed surface area, relative to hydrogen element in the two peaks of hillebrandite, gives a weight ratio hillebrandite/portlandite  $\sim 3.8$  in the sample, if reported to the molecular weight of the phases too.

## 4. Discussion

NMR results are in broad agreement with the XRD, SEM and DTA data. Some methods are relevant to investigate crystalline phases (XRD, SEM and NMR) and NMR is very useful in the case of amorphous or poorly crystallized phases.

The complementary nature of those methods was pointed out for investigations on a sample hydrated at 200 °C under

Table 1

Composition of the  $\text{C}_3\text{S}$  hydrated sample ( $\text{W/C} = 0.44$ ) at 200 °C under 450 bars during 2 months

Phases	Calcite	Portlandite	Jaffeite	Hillebrandite
Weight percentage ( $\pm 1\%$ )	1	13	38	48

a pressure of 450 bars during 2 months. The proposed composition of this  $\text{C}_3\text{S}$  sample is represented on Table 1.

Under the applied conditions of hydration – 200 °C 450 bars and 2 months, there are no more C–S–H. The material matrix is fully crystalline. These results are in close agreement with the pressure and thermal stability of the phases [4]: C–S–H exists at room temperature under atmospheric pressure and is stable under 400 bars up to about 150 °C. jaffeite appears in the first hours of hydration from 100 °C and hillebrandite can be synthesized after a seven days hydration at 200 °C with a  $\text{CaO/SiO}_2$  ratio of 1:2.

## 5. Conclusions

TA, NMR, XRD and SEM techniques were used to study the structure, the morphology and the relative weight of phases formed during a 2 months hydration of  $\text{C}_3\text{S}$  ( $\text{W/C} = 0.44$ ) at 200 °C under 450 bars.

X-ray powder diffraction allowed us to identify the crystalline phases: portlandite, jaffeite, hillebrandite and a small quantity of calcite  $\text{CaCO}_3$ . Both thermal analysis and NMR confirmed these initial qualitative results. Then, the morphology of each phase were observed through scanning electron microscopy. At least, the quantification problem could be solved through thermal analysis and NMR experiments.

Particularly, the amount of portlandite has been computed for our sample by thermal analysis (about 13%). Then,  $^{29}\text{Si}$  NMR single pulse experiment—with respect to the possible longest relaxation time—could quantify the relative amount of the two silicon containing phases, jaffeite and hillebrandite. Finally, due to the  $^1\text{H}$  NMR and CRAMPS sequence, the relative amount of hillebrandite and portlandite could be quantified.

Here, the Rietveld refinement was not used but might be powerful enough to quantify crystallized cementitious phases. For the one particular sample considered, the use of the complementary techniques, previously utilised, allowed the determination of the relative amount of phases (calcite: about 1%, portlandite: about 13%, jaffeite: about 38% and hillebrandite: about 48%). In the future, this process will be generalized to include other samples of hydrated  $\text{C}_3\text{S}$ , in order to determine the phase diagram of  $\text{Ca}_3\text{SiO}_5/\text{H}_2\text{O}$ . The characterisation undertaken provides a basis for further investigation of the properties—more particularly the structure, morphology and later mechanical properties—of hydrated  $\text{C}_3\text{S}$  over a wide range of hydrothermal conditions as found in deep hot wells, up to 1000 bars and 350 °C. In particular, high-resolution solid-state  $^{29}\text{Si}$  NMR has proved to be a valuable tool to dis-

Table 2  
Evaluation of all the methods employed: advantages and limits

Technique	Advantages	Limits
Si-NMR	Local view of a mixture	Long time to obtain quantitatively
H-NMR	Other local “spy” and quantitatively	Setting rather complex
XRD	Detection of crystallized phases	Poorly crystallized phases undetected
SEM	Morphology of phases observed	X-ray analysis not quantitative
Thermal analysis	Detection of crystallized phases	Complex to obtain quantitatively

tinguish phases (even poorly crystallized) formed during hydration of this main component of cement. A comparison of each method used, with advantages and limits, is presented on Table 2. In the future, mechanical probes will be applied to different samples to extend this study and to try to show a correlation between microscopic and macroscopic properties of the different phases found here. We may wonder whether the crystalline phases formed under applied conditions (200 °C–450 bars–2 months) could play the role of a binder, because the usual glue C–S–H, formed as soon as the first hours of setting, have disappeared here.

## Acknowledgments

The authors are grateful to Ciments Français-Italcementi CTG for the tricalcium silicate synthesis, Bernadette Rebours for her help with the XRD-experiments, to Elisabeth Rosenberg for the SEM-observations, to Bruno Bresson for his great help during CRAMPS experiments and to Nicolas Lequeux for access to the pure synthetic phases.

## References

- [1] H.F.W. Taylor, Cement Chemistry, second ed., Thomas Telford Edition, London, 1997.
- [2] G.M.M. Bell, J. Bensted, F.B. Glosser, E.E. Lachowski, D.R. Roberts, S.A. Rodger, Instrumental investigation of hydration of Class J oilwell cement, *Adv. Cem. Res.* 5 (18) (1993) 71–79.
- [3] S. Masse, Synthèse hydrothermale d’hydrates de silicate tricalcique, analyse structurale en phase solide, étude comparative avec les ciments utilisés pour chemiser les puits de pétrole, Thesis, PARIS VI, France, 1993.
- [4] B. Bresson, H. Zanni, Pressure and temperature influence on tricalcium silicate hydration. A  $^1\text{H}$  and a  $^{29}\text{Si}$  NMR study, *J. Chim. Phys.* 95 (1998) 327–331.
- [5] B. Bresson, S. Masse, H. Zanni, C. Noïk, Tricalcium silicate hydration at high temperature. A  $^{29}\text{Si}$  and a  $^1\text{H}$  investigation, in: P. Colombet, A.-R. Grimmer, H. Zanni, P. Sozzani (Eds.), *Nuclear Magnetic Resonance Spectroscopy of Cement-Based Materials*, Springer-Verlag, Berlin, 1998, pp. 333–343.
- [6] E. Lippmaa, M. Mägi, M. Tarmak, W. Wieker, A.R. Grimmer, A high resolution  $^{29}\text{Si}$  NMR Study of the hydration of tricalcium silicate, *Cem. Concr. Res.* 12 (1982) 597–602.
- [7] S.A. Rodger, G.W. Groves, N.J. Clayden, C.M. Dobson, Hydration of tricalcium silicate followed by  $^{29}\text{Si}$  NMR with cross-polarization, *J. Am. Ceram. Soc.* 71 (2) (1988) 91–96.
- [8] B.C. Gerstein, CRAMPS, in: D.M. Grant, R.K. Harris (Eds.), *Encyclopedia of Nuclear Magnetic Resonance*, vol. 3, Wiley, Chichester, England, 1996, pp. 1501–1509.
- [9] B. Bresson, H. Zanni, S. Masse, C. Noïk, Contribution of  $^1\text{H}$  combined rotation and multipulse spectroscopy nuclear magnetic resonance to the study of tricalcium silicate hydration, *J. Mater. Sci.* 32 (1997) 4633–4639.
- [10] D. Heidemann, W. Wieker, Characterization of protons in C–S–H phases by means of high-speed  $^1\text{H}$  MAS NMR investigations, in: P. Colombet, A.-R. Grimmer, H. Zanni, P. Sozzani (Eds.), *Nuclear Magnetic Resonance Spectroscopy of Cement-Based Materials*, Springer-Verlag, Berlin, 1998, pp. 169–180.
- [11] R.E. Marsch, *Acta Crystallogr., Sect. C* 50 (1994) 996.
- [12] E. Schlegel, R. Strienitz, Faserförmige Kalziumsilikathydrate, *Silikat-technik* 41 (Heft 8) (1990) 278–283.
- [13] I. Klur, B. Pollet, J. Virlet, A. Nonat, C–S–H structure evolution with calcium content by multinuclear NMR, in: P. Colombet, A.-R. Grimmer, H. Zanni, P. Sozzani (Eds.), *Nuclear Magnetic Resonance Spectroscopy of Cement-Based Materials*, Springer-Verlag, Berlin, 1998, pp. 119–141.
- [14] G. Engelhardt, D. Michel, *High-Resolution Solid-State NMR of Silicates and Zeolites*, Wiley, New York, 1989.
- [15] G.M.M. Bell, J. Bensted, F.P. Glasser, E.E. Lachowski, D.R. Roberts, M.J. Taylor, Study of calcium silicate hydrates by solid state high resolution  $^{29}\text{Si}$  nuclear magnetic resonance, *Adv. Cem. Res.* 3 (9) (1990) 23–37.
- [16] D. Heidemann, in: P. Colombet, A.R. Grimmer (Eds.), *Application of NMR Spectroscopy to Cement Science*, Guerville, March 1992, Gordon and Breach, Paris, 1994, pp. 77–102.